Engineering Science & Technology
https://ojs.wiserpub.com/index.php/EST/

UNIVERSAL WISER PUBLISHER

Research Article

Modeling and Comparative Analysis of the Compressive Strength of Concretes of Varying Sand Zones Using Scheffe's Theory

D. A. Ekpechi[1*], V. C. Opkalaku-nath[2], U. V. Opara[1], N. I. Ezeaku[3], E. I. Nwankwo[4], C. A. Nwankwo[1], A. Hassan[5], C. O. Osasona[5], D. O. Jackson[6]

[1]Department of Mechanical Engineering, Federal University of Technology, Owerri, Imo State, Nigeria
[2]Department of Civil Engineering, University of Nigeria, Nigeria
[3]Nnamdi Azikiwe University, Awka, Nigeria
[4]Department of Mechanical, Chukwuemeka Odumegwu Ojukwu University, Anambra State, Nigeria
[5]Department of Civil and Environmental Engineering, Kwara State, Nigeria
[6]Department of Civil Engineering, Ladoke Akintola University of Technology, Ogbomosho, Oyo State, Nigeria
E-mail: arinze.ekpechi@futo.edu.ng

Received: 19 August 2024; **Revised:** 7 December 2024; **Accepted:** 17 December 2024

Abstract: The characteristics and application of Scheffe's model to evaluate the data collected from the compressive strength of concrete made with sands from two zones (III and IV) have been investigated. The concrete was developed using Ibagwa River "1" sand (Zone III) and Ibagwa River "2" sand (Zone IV), both obtained from Abakaliki, Ebonyi State, in southern Nigeria. The methodology involves conducting experimental tests to evaluate the compressive strength of concrete cast with different sand types. The resulting experimental data were then analyzed using Scheffe's model, which was validated through Fisher's model. From the results obtained, the Zone III sand indicated a higher compressive strength average of 22.22 N/mm^2 compared to Zone IV's 13.48 N/mm^2. Fisher's test validated the adequacy of Scheffe's model, with total sums of squares of 5.398 (experimental) and 7.002 (model) for Zone III, and 5.26 (experimental) and 6.80 (model) for Zone IV. This implies that Scheffe's model effectively predicts the concrete's compressive strength, with Zone III sand providing more consistent and robust results for structural applications. The meticulous examination of compressive strength provides a nuanced understanding of the comparative performance of concrete mixes, contributing significantly to the optimization of concrete formulation based on sand characteristics. The findings not only enhance the theoretical knowledge of concrete behavior but also offer practical implications for construction practices, reinforcing the applicability and versatility of Scheffe's theory in diverse sand zone scenarios.

***Keywords*:** compressive strength, concrete, Fisher's test, Scheffe's model, optimization

1. Introduction

There is a pressing issue of rapid depletion in natural reserves of conventional crushed rock aggregate and natural river sand, posing a threat to the sustainability of concrete as a construction material [1]. To address these challenges, there is a growing trend in using secondary cementitious materials like fly ash, metakaolin, and silica fumes as partial replacements for cement in concrete production [2]. Additionally, efforts have been made to partially or entirely replace conventional aggregates with materials such as recycled aggregate, polystyrene aggregate, laterite, and quarry dust [3].

DOI: https://doi.org/10.37256/est.6220255525

Numerous studies have explored various types of sand in concrete production. Zone II sand is favoured for its gradation, which enhances workability and strength development [4]. Zone III sand, characterized by finer particles, is often used where higher compaction is required [5]. Sea sand, though abundant, is limited by high chloride content, which can corrode reinforcement [6]. Pit sand, commonly found in excavation sites, contains larger particles but may require washing to remove clay and silt impurities [7]. Concrete sand, widely available in construction sites, is valued for consistent particle size but may lack the strength properties of river sand [7]. Utility sand and manufactured sand (M-sand) are eco-friendly alternatives, with M-sand specifically engineered to mimic the properties of natural sand, though it may require advanced processing to eliminate angularity issues [8].

River sand, such as Ibagwa River sand, remains integral to concrete production due to its naturally rounded particles, excellent gradation, and clean composition, which reduce water demand and improve concrete workability [9]. Despite concerns about the depletion of natural reserves, this study emphasizes the geological uniqueness of Ibagwa River sand, which exhibits optimal grading and particle texture, justifying its selection. Moreover, its local availability minimizes transportation emissions, aligning with sustainability efforts [10]. A balanced approach, including sustainable mining practices and integrating alternatives like M-sand, is essential to addressing the depletion issue [11].

Some notable research have been done using models to build standards for structural engineering systems. For example, Edidiong et al. [12] investigated the impact of the fine aggregate content of crushed recycled-ceramic tiles (CRT) on the compressive strength of concrete. Scheffe's second-degree polynomial models were formulated for compressive strength, slump height, and cost of CRT concrete. The findings reveal that the incorporation of CRT as fine aggregate enhances the compressive strength of concrete. This improvement is directly proportional to its content. The study recommends replacing conventional fine aggregate with CRT up to 100% in concrete production. Additionally, the formulated models can predict compressive strength, slump, and cost of CRT concrete when the mix ratio is known, and vice versa. Adequacy tests, including analysis of variance and normal probability plots of model residuals, were conducted. These tests confirm the models' reliability at a 95% confidence level. Using the model equations, sample optimization was performed to identify the most economical mix for predefined criteria. The results were promising. The study suggests that similar optimizations can be conducted using the formulated model equations. These optimizations can meet various criteria for the modeled responses [13].

Akeke et al. [14] enhanced the mechanical properties of concrete by incorporating palm oil fuel ash (POFA) and optimizing the mixture using Scheffe's design. POFA, a supplementary cementitious material, has garnered attention for its environmental benefits. Employing a (5, 2) simplex-lattice design, the study systematically optimized mixture proportions based on response parameters. Laboratory tests on the mechanical behavior of concrete were conducted using computed mixture ratios after 28 days of hydration. The results demonstrated that the maximum flexural strength (8.84 N/mm^2) and compressive strength (31.16 N/mm^2) were achieved with a mix ratio of 0.65: 0.54: 2.3: 3.96: 0.35 for cement, water, coarse aggregate, fine aggregate, and POFA. Additionally, the maximum splitting tensile strength reached 8.84 N/mm^2 with a mix ratio of 0.62: 0.55: 2.09: 3.86: 0.38 for the same components. Conversely, the minimum flexural, splitting tensile, and compressive strength within the experimental factor space were 4.25, 2.08, and 19.82 N/mm^2, respectively. Satisfactory mechanical strength performance was observed with a 35 percent replacement of POFA in the concrete mixture. The developed mathematical model was statistically validated using analysis of variance (ANOVA) at a 95% confidence interval, demonstrating satisfactory prediction performance. Overall, the findings provide valuable insights into optimizing POFA-blended concrete for enhanced mechanical performance, suggesting potential sustainable solutions for the construction industry [15].

Enang and Ewa [16] used laterite-quarry dust cement blocks, which are masonry units produced by fully replacing natural sand with a suitable mix of laterite and quarry dust. The static modulus of elasticity is a crucial parameter for predicting the structural behavior of these blocks under load conditions. It determines the distribution of deformations and displacements in concrete and similar structural elements. The research introduces a mathematical model formulated through a mixture experiment to predict the static modulus of elasticity for Laterite-Quarry Dust Blocks. The model undergoes testing for lack of fit and is deemed adequate for its intended purpose.

Arimanwa et al. [17] evaluated the impact of the chemical composition of ordinary portland cement (OPC) on concrete compressive strength in South Eastern Nigeria. Utilizing Scheffe's simplex technique, five models are formulated to predict compressive strength based on known mix proportions or vice versa. The study aims to simplify the selection of concrete mix proportions, providing a straightforward method for obtaining compressive strength

information for various OPC brands. Laboratory experiments involve 300 sample cubes, and the results indicate that all cement samples comply substantially with relevant British Standard Specifications. The chemical composition of cement, along with mix proportions, influences the compressive strength of the resulting concrete. Cement Sample B exhibits the highest 28th-day compressive strength at 27.96 N/mm^2. The conclusion highlights that cement with similar chemical characteristics produces comparable compressive strength. Cement Sample B is the optimal choice, particularly for applications prioritizing compression resistance and strength development rate [18].

The identified research gap lies in the absence of a comprehensive and unified approach to predictive modeling and optimization in concrete technology. While individual studies focus on specific components, such as recycled ceramic tiles, palm oil fuel ash, and laterite-quarry dust, there is no research yet on the application of Scheffe's model, validated with Fisher's statistical model on the experimental compressive strength data from two-layer Ibagwa river sand from southern part Nigeria, in enhancing the structural strength of concrete.

2. Materials and method

2.1 *Materials*

Several contemporary methodologies have been applied in concrete mix design. The Taguchi-GRA method integrates statistical analysis and optimization to enhance mix proportions while balancing cost and performance [19]. Response surface methodology (RSM) is another powerful tool that uses mathematical modelling to optimize concrete properties through factor-response relationships, allowing for efficient design iterations [20]. Scheffe's theory, however, stands out for its simplicity and robustness in handling mixture proportions through polynomial regression, offering clear predictions for properties like compressive strength [21].

In this study, Scheffe's theory was chosen due to its ability to effectively model the non-linear interactions of concrete constituents, particularly with variations in sand types. Unlike Taguchi-GRA and RSM, which require extensive computational resources and are better suited for multi-response optimization, Scheffe's approach aligns with the study's primary focus on predicting compressive strength accurately with a concise dataset. This choice ensures reliability and applicability, meeting the research objectives while maintaining methodological clarity.

Ordinary portland cement (OPC Unicem) was purchased from Kenyatta Market in Enugu State. Fine aggregate (river sand) was obtained from two sources: Ibagwa River "1" sand (Zone III) and Ibagwa River "2" sand (Zone IV), both located in Enugu State. Coarse aggregates with a size of 20 mm were sourced from Abakaliki, Ebonyi State, in the southern part of Nigeria. Water was sourced from the laboratory reservoir. Table 1 lists the equipment used in the preparation and experimental phases of the research.

Table 1. Equipment and apparatus used in sample preparation and in the various tests

S/N	Item	Specification	Usage
1	Sieve	Aperture Sizes: 4.75 mm, 2.36 mm, 1.18 mm, 600 µm, 300 µm, 150 µm	Particle size distribution analysis
2	Truncated cone	Height: 300 mm, Base Diameter: 200 mm, Top Diameter: 100 mm	Slump test for workability
3	Tamping rod	Diameter: 16 mm, Length: 600 mm	Slump test for compaction
4	Scoop	Capacity: 1,000 ml	Slump test for adding concrete to cone
5	Ruler	Length: 300 mm	Measuring slump test results
6	Hydration container	Capacity: 100 liters	Curing concrete samples
7	Psychomotor	Range: 0.01-1.00 specific gravity	Specific gravity tests
8	Oven	Temperature range: up to 110 °C	Drying samples
9	Compression testing machine	Capacity: 2,000 kN, Digital display	Determining compressive strength of concrete samples

2.2 *Method*

2.2.1 *Experimental phase*

All practical experiments were conducted at the Vengen Geotechnical Engineering Services Concrete Laboratory. Sand samples were checked to ensure they were free from impurities, dried, and collected at room temperature. Two mixes were prepared, one using river sand from Zone III and from Zone IV. Concrete samples were cast using Ordinary Portland Cement (UNICEM) as binder in a mix ratio of 1 : 2 : 4, and the water/cement ratio was adjusted according to the suitability for each mix.

The particle size distribution of the fine aggregate was determined. Samples were washed, dried, sieved, and weights were recorded for each sieve. The fineness modulus and zoning chart indicated suitability for concrete (Zone II). The workability of the concrete mix was assessed using a truncated cone, tamping rod, scoop, and ruler. Manual mixing was conducted, with quantities measured in kilograms. Precautions were taken to avoid excessive hand pressure on sieves and spillage, and to maintain drying temperatures below 110 °C. Ordinary Portland Cement, river sand, and 20 mm crushed coarse aggregates were used. Concrete cubes were prepared using a designed nominal concrete mix, and curing was done in a hydration container filled with water. Tests were conducted at 7, 14, 21, and 28 days.

Table 2 presents the weights of different components used in the concrete mix. Typically, these components in a concrete mix include cement, fine aggregate of sand, coarse aggregate of gravel or crushed stone, and water.

Table 2. Compositions of the experimental samples

Specimen label	Cement (Z1)	Fine aggregate	Coarse aggregate	Water
C1	0.53 kg	1.00 kg	1.70 kg	3.625 kg
C2	0.55 kg	1.00 kg	1.85 kg	3.80 kg
C3	0.60 kg	1.00 kg	2.00 kg	4.00 kg
C4	0.65 kg	1.00 kg	2.20 kg	4.20 kg
C5	0.70 kg	1.00 kg	2.35 kg	4.40 kg
C6	0.75 kg	1.00 kg	2.50 kg	4.60 kg
C7	0.80 kg	1.00 kg	2.70 kg	4.80 kg
C8	0.85 kg	1.00 kg	2.85 kg	5.00 kg
C9	0.90 kg	1.00 kg	3.00 kg	5.20 kg
C10	0.95 kg	1.00 kg	3.20 kg	5.40 kg

2.2.2 *Application of Scheffe's model*

In this work, Scheffe's mathematical model method was used to formulate the optimization models and was based on simplex lattice design [22]-[26]. According to Imoh et al. [27], the sum of all mixture components in a factor space based on the application of this model must be equal to one.

$$\text{Therefore, } x_1 + x_2 + x_3 + \ldots + x_q \pi^R + x_q = 1 \tag{1}$$

$$\text{Hence, } \sum_{i=1}^{q} xi = 1 \tag{2}$$

Where q is the number of points of a mixture ranging from 1 to q.

x_i is the proportion of the ith component in the mixture. The polynomial function will be used to formulate the model. The manner of coefficient in of the polynomial according to Scheffe's is given as

$$n = \frac{(q+m-1)!}{(q-1)!m!} \tag{3}$$

Where M is the degree of the polynomial. Thus, for $q = 4$ and $m = 2$, substituting the values in equation (3),

$$n = \frac{(4+2-1)!}{(4-1)!2!} = \frac{5!}{3!2!} = 10$$

Hence, $n = 10$ signifies that, for a (4, 2) simplex design, we have 10 coefficients of the polyniminal function, corresponding to 10 experimental runs.

The concrete mixture consists of four components: water, cement, sand, and crushed stone sourced from different locations.

The space to use in the analysis will be $(q - 1)$ dimensional simplex lattice equal to 3D factor space [28]-[29] as shown in Figure 1.

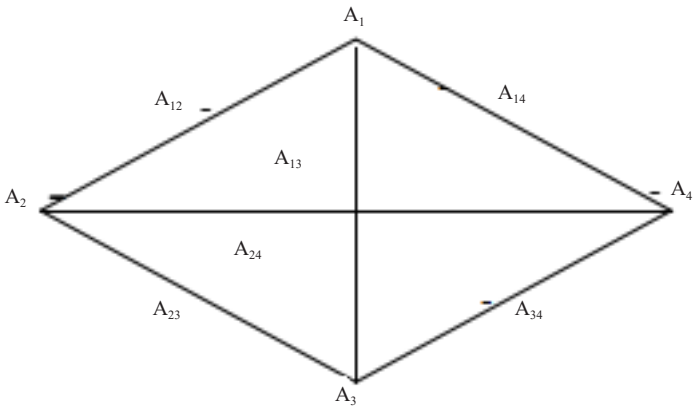

Figure 1. A (4,2) Scheffe's simplex lattice with 10 experimental runs

The quantities of the form pseudo components at these ten points are as follows:

$$A_1(1 \quad 0 \quad 0 \quad 0)$$

$$A_2(0 \quad 1 \quad 0 \quad 0)$$

$$A_3(0 \quad 0 \quad 1 \quad 0)$$

$$A_4(0 \quad 0 \quad 0 \quad 1)$$

$$A_{12}(\frac{1}{2} \quad \frac{1}{2} \quad 0 \quad 0)$$

$$A_{13}(\frac{1}{2} \quad 0 \quad \frac{1}{2} \quad 0)$$

$$A_{14}(\frac{1}{2} \quad 0 \quad 0 \quad \frac{1}{2})$$

$$A_{23}(0 \quad \frac{1}{2} \quad \frac{1}{2} \quad 0)$$

$$A_{24}(0 \quad \frac{1}{2} \quad 0 \quad \frac{1}{2})$$

$$A_{34}(0 \quad 0 \quad \frac{1}{2} \quad \frac{1}{2})$$

Onyia et al. [26] refer to responses as the properties of fresh and hardened concrete. According to Imoh et al. [27], these responses can be expressed as a polynomial function of pseudo component. The form-pseudo component mixture is given below:

$$\mathrm{Y} = b_0 + b_1x_1 + b_2x_2 + b_3x_3 + b_4x_4 + b_{11}x_1^2 + b_{12}x_1x_2 + b_{13}x_1x_3 +$$

$$b_{14}x_1x_4 + b_{22}x_2^2 + b_{23}x_2x_3 + b_{24}x_2x_4 + b_{33}x_3^2 + b_{34}x_3x_4 + b_{44}x_4^2 + \propto \tag{4}$$

The term α is the random error, which represents the combined effects of variables not included in the model.

$$\text{Hence, } x_1 + x_2 + x_3 + x_4 = 1 \tag{5}$$

$$\text{Multiplying equation (5) by } b_0 \text{ will be } b_0x_1 + b_0x_2 + b_0x_3 + b_0x_4 = b_0 \tag{6}$$

Multiplying equation (5) by x_1, x_2, x_3, and x_4 in succession gives

$$x_1^2 + x_1x_2 + x_1x_3 + x_1x_4 = x_1 \tag{7}$$

$$x_1x_2 + x_2^2 + x_2x_3 + x_2x_4 = x_2 \tag{8}$$

$$x_1x_3 + x_2x_3 + x_3^2 + x_3x_4 = x_3 \tag{9}$$

$$x_1x_4 + x_2x_4 + x_3x_4 + x_4^2 = x_4 \tag{10}$$

Rearranging equations (7)-(10) in terms of x_i will become

$$x_1^2 = x_1 - x_1x_2 - x_1x_3 - x_1x_4 \tag{11}$$

$$x_2^2 = x_2 - x_1x_2 - x_2x_3 - x_2x_4 \tag{12}$$

$$x_3^2 = x_3 - x_1x_3 - x_2x_3 - x_3x_4 \tag{13}$$

$$x_4^2 = x_4 - x_1x_4 - x_2x_4 - x_3x_4 \tag{14}$$

Substituting equation (6) and equations (11)-(14) into equation (4)

$$\begin{aligned} Y = {} & b_0x_1 + b_0x_2 + b_ox_3 + b_0x_4 + b_1x_1 + b_2x_2 + b_3x_3 + b_4x_4 - b_{11}x_1 - b_{11}x_1x_2 \\ & - b_{11}x_1x_3 - b_{11}x_1x_4 + b_{12}x_1x_2 - b_5x_1x_2 - b_{14}x_1x_4 + b_{22}x_2 + b_{22}x_1x_2 \\ & - b_{22}x_2x_3 - b_{22}x_2x_4 + b_{23}x_2x3 + b_{24}x_2x_4 + b_{33}x_5 - b_{33}x_1x_3 - b_{33}x_2x_3 \\ & + b_{33}x_3x_4 + b_{34}x_3x_4 + b_{44}x_4 - b_{44}x_1x4 - b_{44}xx_2 - b_{44}x_3x_4 \end{aligned} \tag{15}$$

Rearranging equation (15) and bringing like terms together will give

$$\begin{aligned} Y = {} & \left(b_o + b_1 + b_{11}\right)x_1 + \left(b_o + b_2 + b_{22}\right)x_2 + \left(b_o + b_3 + b_{33}\right)x_3 + \left(b_o + b_4 + b_{44}\right)x_4 \\ & + \left(b_{12} - b_{11} - b_{22}\right)x_1x_2 + \left(b_{13} - b_{11} - b_{33}\right)x_1x_3 + \left(b_{14} - b_{11} - b_{44}\right)x_1x_4 \\ & + \left(b_{23} - b_{22} - b_{33}\right)x_2x_3 + \left(b_{24} - b_{22} - b_{44}\right)x_2x_4 + \left(b_{34} - b_{33} - b_{44}\right)x_3x_4 \end{aligned} \tag{16}$$

It is worthy of note here that when constants are added together, another constant will result. Hence, the summation terms in parathesis in equation (16) will be replaced with $\propto$ as

$$\propto_1 = b_o + b_1 + b_{11}$$

$$\propto_2 = b_o + b_2 + b_{22}$$

$$\propto_3 = b_o + b_3 + b_{33}$$

$$\propto_4 = b_o + b_4 + b_{44}$$

$$\propto_{12} = b_{12} - b_{11} - b_{22}$$

$$\propto_{13} = b_{13} - b_{11} - b_{33}$$

$$\propto_{14} = b_{14} - b_{11} - b_{44}$$

$$\propto_{23} = b_{23} - b_{22} - b_{33}$$

$$\propto_{24} = b_{24} - b_{22} - b_{44}$$

$$\propto_{34} = b_{34} - b_{33} - b_{44} \tag{17}$$

Substituting equation (17) in equation (16)

$$Y = \propto_1 x_1 + \propto_2 x_2 + \propto_3 x_3 + \propto_4 x_4 + \propto_{12} x_1x_2 + \propto_{13} x_1x_3 + \propto_{14} x_1x_4$$

$$+ \propto_{23} x_2x_3 + \propto_{24} x_2x_4 + \propto_{34} x_2x_4 + \varepsilon \quad (18)$$

Equation (18) can be rewritten as $Y = \ddot{y} + \varepsilon$
Where ε = standard error

$$\ddot{y} = \propto_1 x_1 + \propto_2 x_2 + \propto_3 x_3 + \propto_4 x_4 + \propto_{12} x_1x_2 + \propto_{13} x_1x_3$$

$$+ \propto_{14} x_1x_4 + \propto_{23} x_2x_3 + \propto_{24} x_2x_4 + \propto_{34} x_3x_4 \quad (19)$$

Equation (19) is the Scheffe's (4.2) lattice polynomial equation. These responses are constant and are determined by carrying out laboratory practicals. A total of ten (10) of such practical tests will be carried out to correspond to the ten coefficients of equation (19) can be expressed in the form:

$$\ddot{y} = \sum_{i=1}^{4} \propto_i x_i + \sum_{1 \le i \le j \le 4} \propto_{ij} x_i x_j \quad (20)$$

Equation (20) can be seen as the response to the pure components, i, and the binary mixture components, j. At each vertex of the factor space, the component $x_2 = 1$ while other components are all equal to acro. At the midpoint of all the border lines of the factor space, the two components x_2 and x_j are equal to $\frac{1}{2}$ each, while most of the components are equal to zero. The response at each point on the factor space is obtained as follows using equation (19) for the pure components.

$$Y_1 = \propto_1 \quad (21)$$

$$Y_2 = \propto_2 \quad (22)$$

$$Y_3 = \propto_3 \quad (23)$$

$$Y_4 = \propto_4 \quad (24)$$

2.2.3 *Optimum point*

The optimum point is the point in the factor space that produces the mixture proportion yielding the most desired property [30]. According to Ubachukwu and Okafor [31], different optimum points exist in the imaginary space, and their identification depends on various factors and considerations. For a particular optimum point desired to meet the considerations in mind, it is important to use a defined factor space to enclose. Failure to do so may result in the optimum point lying outside the defined boundaries [32].

The conservancies of this are that the model cannot produce the optimum point to define a factor space that will enclose the desired optimum point. Instead, previous experiments and past experience will come into play. Where there is no past experience or previous experimental data, trial mixes can be made, which serve as fair guide to the optimum point. The actual mixture proportions required at these points correspond to the four mixture proportions located at the four vertices of the factor space. These four proportions will define the revised factor space that will entrap or close the desired optimum points. Listed below are the actual mixture proportion at the four vertices [33].

$$A_1(0.5:1:2:4)$$

$$A_2(0.52:1:1.8:3.7)$$

$$A_3(0.54:1:1.6:3.5)$$

$$A_4(0.56:1:1.4:3.3)$$

The proportions correspond to w/c ratio, cements, sand, and crushed granite. According to Agunwamba et al. [34], Scheffe's model defines the relationship between actual and pseudo components as follows:

$$Z = AX \tag{25}$$

Where Z is the actual component, X is the pseudo component, and A is the coefficient of the relationship. The value of matrix A will be determined from the first four real mix ratios using equations (25), rearranging equation (25):

$$A = X^{-1}Z \tag{26}$$

The coefficient of the relationship

$$[A] = \begin{pmatrix} a_{11} & a_{12} & a_{13} & a_{14} \\ a_{21} & a_{22} & a_{23} & a_{24} \\ a_{31} & a_{32} & a_{33} & a_{34} \\ a_{41} & a_{42} & a_{43} & a_{44} \end{pmatrix} \tag{27}$$

The actual components for the first four runs

$$Z_1\ [0.50:1:2:4]$$

$$Z_2\ [0.52:1:1:1.8:3.7]$$

$$Z_3\ [0.54:1:1.6:3.5]$$

$$Z_4\ [0.56:1:1.4:3.3]$$

The pseudo components for the first four are

$$X_1\ [1:0:0:0:0]$$

$$X_2\ [0:1:1:0:0]$$

$$X_3\ [0:0:0:1:0]$$

$$X_4\ [0:0:0:0:0]$$

Expressing equation (28) in matrix form

$$\begin{pmatrix} Z_1 \\ Z_2 \\ Z_3 \\ Z_4 \end{pmatrix} = \begin{pmatrix} a_{11} & a_{12} & a_{13} & a_{14} \\ a_{21} & a_{22} & a_{23} & a_{24} \\ a_{31} & a_{32} & a_{33} & a_{34} \\ a_{41} & a_{42} & a_{43} & a_{44} \end{pmatrix} \begin{pmatrix} x_1 \\ x_2 \\ x_3 \\ x_4 \end{pmatrix} \tag{28}$$

For the first run, A_1

$$\begin{pmatrix} 0.50 \\ 1.00 \\ 2.00 \\ 4.00 \end{pmatrix} = \begin{pmatrix} a_{11} & a_{12} & a_{13} & a_{14} \\ a_{21} & a_{22} & a_{23} & a_{24} \\ a_{31} & a_{32} & a_{33} & a_{34} \\ a_{41} & a_{42} & a_{43} & a_{44} \end{pmatrix} \begin{pmatrix} 1 \\ 0 \\ 0 \\ 0 \end{pmatrix} \tag{29}$$

This gives $a_{11} = 0.50$, $a_{21} = 1.00$, $a_{31} = 2.00$, and $a_{41} = 4.00$.
For the second run, A_2

$$\begin{pmatrix} 0.52 \\ 1.00 \\ 1.80 \\ 3.70 \end{pmatrix} = \begin{pmatrix} a_{11} & a_{12} & a_{13} & a_{14} \\ a_{21} & a_{22} & a_{23} & a_{24} \\ a_{31} & a_{32} & a_{33} & a_{34} \\ a_{41} & a_{42} & a_{43} & a_{44} \end{pmatrix} \begin{pmatrix} 0 \\ 1 \\ 0 \\ 0 \end{pmatrix} \tag{30}$$

Hence, $a_{12} = 0.52$, $a_{22} = 1.00$, $a_{32} = 1.80$, and $a_{42} = 3.70$.
For the third run, A_3

$$\begin{pmatrix} 0.54 \\ 1.00 \\ 1.60 \\ 3.50 \end{pmatrix} = \begin{pmatrix} a_{11} & a_{12} & a_{13} & a_{14} \\ a_{21} & a_{22} & a_{23} & a_{24} \\ a_{31} & a_{32} & a_{33} & a_{34} \\ a_{41} & a_{42} & a_{43} & a_{44} \end{pmatrix} \begin{pmatrix} 0 \\ 0 \\ 1 \\ 0 \end{pmatrix} \tag{31}$$

Therefore, $a_{13} = 0.54$, $a_{23} = 1.00$, $a_{33} = 1.60$, and $a_{43} = 3.50$.
For the fourth run, A_4

$$\begin{pmatrix} 0.56 \\ 1.00 \\ 1.40 \\ 3.30 \end{pmatrix} = \begin{pmatrix} a_{11} & a_{12} & a_{13} & a_{14} \\ a_{21} & a_{22} & a_{23} & a_{24} \\ a_{31} & a_{32} & a_{33} & a_{34} \\ a_{41} & a_{42} & a_{43} & a_{44} \end{pmatrix} \begin{pmatrix} 0 \\ 0 \\ 0 \\ 1 \end{pmatrix} \tag{32}$$

This gives $a_{14} = 0.56$, $a_{24} = 1.00$, $a_{34} = 1.40$, and $a_{44} = 3.30$. Substituting the values of the constants, the matrix $[A]$ is formed.

$$[A] = \begin{bmatrix} 0.50 & 0.52 & 0.54 & 0.56 \\ 1.00 & 1.00 & 1.00 & 1.00 \\ 2.00 & 1.80 & 1.60 & 1.40 \\ 4.00 & 3.70 & 3.50 & 3.30 \end{bmatrix} \tag{33}$$

With the coefficient of relation (A) known and the pseudo-components (Y_{12} to Y_{34}) also determined, the actual components (Z) can be obtained.

Fifth run, A_{12}

$$\begin{pmatrix} Z_1 \\ Z_2 \\ Z_3 \\ Z_4 \end{pmatrix} = \begin{pmatrix} 0.50 & 0.52 & 0.54 & 0.56 \\ 1.00 & 1.00 & 1.00 & 1.00 \\ 2.0 & 1.80 & 1.60 & 1.40 \\ 4.00 & 3.70 & 3.50 & 3.30 \end{pmatrix} \begin{pmatrix} 0.50 \\ 0.50 \\ 0 \\ 0 \end{pmatrix}$$

$$Z_1 = (0.50 \times 0.50) + (0.52 \times 0.50) = 0.51$$

$$Z_2 = (1.00 \times 0.50) + (1.00 \times 0.50) = 1$$

$$Z_3 = (2.00 \times 0.50) + (1.80 \times 0.50) = 1.9$$

$$Z_4 = (4.00 \times 0.50) + (3.70 \times 0.50) = 3.85 \quad (34)$$

For the sixth run, A_{13}

$$\begin{pmatrix} Z_1 \\ Z_2 \\ Z_3 \\ Z_4 \end{pmatrix} = \begin{pmatrix} 0.50 & 0.52 & 0.54 & 0.56 \\ 1.00 & 1.00 & 1.00 & 1.00 \\ 2.0 & 1.80 & 1.60 & 1.40 \\ 4.00 & 3.70 & 3.50 & 3.30 \end{pmatrix} \begin{pmatrix} 0.50 \\ 0 \\ 0.50 \\ 0 \end{pmatrix}$$

$$Z_1 = (0.50 \times 0.50) + (0.54 \times 0.50) = 0.52$$

$$Z_2 = (1.00 \times 0.50) + (1.00 \times 0.50) = 1$$

$$Z_3 = (2.00 \times 0.50) + (1.60 \times 0.50) = 1.80$$

$$Z_4 = (4.00 \times 0.50) + (3.50 \times 0.50) = 3.75 \quad (35)$$

For the seventh run, A_{14}

$$\begin{pmatrix} Z_1 \\ Z_2 \\ Z_3 \\ Z_4 \end{pmatrix} = \begin{pmatrix} 0.50 & 0.52 & 0.54 & 0.56 \\ 1.00 & 1.00 & 1.00 & 1.00 \\ 2.00 & 1.80 & 1.60 & 1.40 \\ 4.00 & 3.70 & 3.50 & 3.30 \end{pmatrix} \begin{pmatrix} 0.50 \\ 0 \\ 0 \\ 0.50 \end{pmatrix}$$

$$Z_1 = (0.50 \times 0.50) + (0.56 \times 0.50) = 0.53$$

$$Z_2 = (1.00 \times 0.50) + (1.40 \times 0.56) = 1.70$$

$$Z_3 = (2.00 \times 0.50) + (1.60 \times 0.50) = 1.80$$

$$Z_4 = (4.00 \times 0.50) + (3.30 \times 0.50) = 3.65 \quad (36)$$

For the eighth run, A_{23}

$$\begin{pmatrix} Z_1 \\ Z_2 \\ Z_3 \\ Z_4 \end{pmatrix} = \begin{pmatrix} 0.50 & 0.52 & 0.54 & 0.56 \\ 1.00 & 1.00 & 1.00 & 1.00 \\ 2.00 & 1.80 & 1.60 & 1.40 \\ 4.00 & 3.70 & 3.50 & 3.30 \end{pmatrix} \begin{pmatrix} 0 \\ 0.50 \\ 0.50 \\ 0 \end{pmatrix}$$

$$Z_1 = (0.52 \times 0.5) + (0.54 \times 0.5) = 0.53$$

$$Z_2 = (1.00 \times 0.5) + (1.00 \times 0.50) = 1$$

$$Z_3 = (1.50 \times 0.5) + (1.60 \times 0.5) = 1.70$$

$$Z_4 = (3.70 \times 0.5) + (3.50 \times 0.5) = 3.60 \quad (37)$$

Ninth run, A_{24}

$$\begin{pmatrix} Z_1 \\ Z_2 \\ Z_3 \\ Z_4 \end{pmatrix} = \begin{pmatrix} 0.50 & 0.52 & 0.54 & 0.56 \\ 1.00 & 1.00 & 1.00 & 1.00 \\ 2.00 & 1.30 & 1.60 & 1.40 \\ 4.00 & 3.70 & 3.50 & 3.30 \end{pmatrix} \begin{pmatrix} 0 \\ 0.50 \\ 0 \\ 0.50 \end{pmatrix}$$

$$Z_1 = (0.52 \times 0.5) + (0.56 \times 0.5) = 0.54$$

$$Z_2 = (1.00 \times 0.5) + (1.00 \times 0.5) = 1$$

$$Z_3 = (1.80 \times 0.5) + (1.40 \times 0.5) = 1.60$$

$$Z_4 = (370 \times 0.5) + (3.3 \times 0.5) = 3.50 \quad (38)$$

Tenth run, A_{34}

$$\begin{pmatrix} Z_1 \\ Z_2 \\ Z_3 \\ Z_4 \end{pmatrix} = \begin{pmatrix} 0.50 & 0.52 & 0.54 & 0.56 \\ 1.00 & 1.00 & 1.00 & 1.00 \\ 2.00 & 1.80 & 1.60 & 1.40 \\ 4.00 & 3.70 & 3.50 & 3.30 \end{pmatrix} \begin{pmatrix} 0 \\ 0 \\ 0.50 \\ 0.50 \end{pmatrix}$$

$$Z_1 = (0.54 \times 0.5) + (0.56 \times 0.5) = 0.55$$

$$Z_2 = (1.00 \times 0.5) + (1.00 \times 0.5) = 1$$

$$Z_3 = (1.60 \times 0.5) + (1.40 \times 0.5) = 1.50$$

$$Z_4 = (3.50 \times 0.5) + (3.30 \times 0.5) = 3.40 \quad (39)$$

The pseudo components and corresponding actual components at different points on the factor space are summarized in Table 3.

Table 3. Mixture proportion of experiment

	Actual					Pseudo			
S/N	Z_1	Z_2	Z_3	Z_4	Response	x_1	x_2	x_3	x_4
1	0.50	1	2	4	Y_1	1	0	0	0
2	0.52	1	1.80	3.70	Y_2	0	1	0	0
3	0.54	1	1.60	3.50	Y_3	0	0	1	0
4	0.56	1	1.40	3.30	Y_4	0	0	0	1
5	0.51	1	1.90	3.85	Y_{12}	0.5	0.5	0	0
6	0.52	1	1.80	3.75	Y_{13}	0.5	0	0.5	0
7	0.53	1	1.70	3.65	Y_{14}	0.5	0	0	0.5
8	0.53	1	1.70	3.60	Y_{23}	0	0.5	0.5	0
9	0.54	1	1.60	3.50	Y_{24}	0	0.5	0	0.5
10	0.55	1	1.50	3.40	Y_{34}	0	0	0.5	0.5

Where x_1 is water/cement ratio, x_2 is cement (Opc), x_3 is sand, and x_4 is crushed granite.

2.2.4 *Control point of the system*

Control points for test of adequacy for the matrix [A] is further used to obtained the corresponding properties for the control points by applying equation (39) with the pseudo components set by the sum of one of the mixture component constraints [35]. Following the applied model by Agunwamba et al. [34], the ten control points required to confirm the adequacy of the models are C_1, C_2, C_3, C_4, C_{12}, C_{13}, C_{14}, C_{23}, C_{24}, and C_{34} respectively.

Control point C_1

$$\begin{pmatrix} Z_1 \\ Z_2 \\ Z_3 \\ Z_4 \end{pmatrix} = \begin{pmatrix} 0.50 & 0.52 & 0.54 & 0.56 \\ 1.00 & 1.00 & 1.00 & 1.00 \\ 2.00 & 1.80 & 1.60 & 1.40 \\ 4.00 & 3.70 & 3.50 & 3.30 \end{pmatrix} \begin{pmatrix} 0.25 \\ 0.25 \\ 0.25 \\ 0.25 \end{pmatrix}$$

$$Z_1 = (0.50 \times 0.25) + (0.52 \times 02.5) + (0.54 \times 0.25) + (0.56 \times 02.5) = 0.53$$

$$Z_2 = (1.00 \times 0.5) + (1.00 \times 0.5) + (0.50 \times 0.25) + (0.52 \times 02.5) = 1$$

$$Z_3 = (2.00 \times 0.25) + (1.80 \times 0.25) + (1.60 \times 0.25) + (1.40 \times 02.5) = 1.70$$

$$Z_4 = (4.00 \times 0.25) + (3.70 \times 0.25) + (3.50 \times 0.25) + (5.30 \times 02.5) = 3.625 \quad (40)$$

Control point C_2

$$\begin{pmatrix} Z_1 \\ Z_2 \\ Z_3 \\ Z_4 \end{pmatrix} = \begin{pmatrix} 0.50 & 0.52 & 0.54 & 0.56 \\ 1.00 & 1.00 & 1.00 & 1.00 \\ 2.00 & 1.80 & 1.60 & 1.40 \\ 4.00 & 3.70 & 3.50 & 3.30 \end{pmatrix} \begin{pmatrix} 0.50 \\ 0.25 \\ 0.25 \\ 0 \end{pmatrix}$$

$$Z_1 = (0.50 \times 0.50) + (0.52 \times 02.5) + (0.54 \times 0.25) = 0.515$$

$$Z_2 = (1.00 \times 0.50) + (1.00 \times 0.25) + (0.00 \times 0.25) = 1$$

$$Z_3 = (2.00 \times 0.50) + (1.80 \times 0.25) + (1.60 \times 0.25) = 1.85$$

$$Z_4 = (4.00 \times 0.50) + (3.70 \times 0.25) + (3.50 \times 0.25) = 3.80 \quad (41)$$

Control point C_3

$$\begin{pmatrix} Z_1 \\ Z_2 \\ Z_3 \\ Z_4 \end{pmatrix} = \begin{pmatrix} 0.50 & 0.52 & 0.54 & 0.56 \\ 1.00 & 1.00 & 1.00 & 1.00 \\ 2.00 & 1.80 & 1.60 & 1.40 \\ 4.00 & 3.70 & 3.50 & 3.30 \end{pmatrix} \begin{pmatrix} 0 \\ 0.25 \\ 0.25 \\ 0.50 \end{pmatrix}$$

$$Z_1 = (0.52 \times 0.25) + (0.54 \times 0.02.5) + (0.56 \times 0.5) = 0.545$$

$$Z_2 = (1.00 \times 0.25) + (1.00 \times 0.25) + (0.00 \times 0.5) = 1$$

$$Z_3 = (1.80 \times 0.25) + (1.60 \times 0.25) + (1.40 \times 0.5) = 1.55$$

$$Z_4 = (3.70 \times 0.25) + (3.50 \times 0.25) + (3.30 \times 0.5) = 3.45 \quad (42)$$

Control point C_4

$$\begin{pmatrix} Z_1 \\ Z_2 \\ Z_3 \\ Z_4 \end{pmatrix} = \begin{pmatrix} 0.50 & 0.52 & 0.54 & 0.56 \\ 1.00 & 1.00 & 1.00 & 1.00 \\ 2.00 & 1.80 & 1.60 & 1.40 \\ 4.00 & 3.70 & 3.50 & 3.30 \end{pmatrix} \begin{pmatrix} 0 \\ 0.25 \\ 0 \\ 0.75 \end{pmatrix}$$

$$Z_1 = (0.52 \times 0.25) + (0.56 \times 075) = 0.55$$

$$Z_2 = (1.00 \times 0.25) + (1.00 \times 0.75) = 1$$

$$Z_3 = (1.80 \times 0.25) + (1.40 \times 0.75) = 1.50$$

$$Z_4 = (3.70 \times 0.25) + (3.30 \times 0.75) = 3.40 \tag{43}$$

Control Point C_{12}

$$\begin{pmatrix} Z_1 \\ Z_2 \\ Z_3 \\ Z_4 \end{pmatrix} = \begin{pmatrix} 0.50 & 0.52 & 0.54 & 0.56 \\ 1.00 & 1.00 & 1.00 & 1.00 \\ 2.00 & 1.80 & 1.50 & 1.40 \\ 4.00 & 3.70 & 3.50 & 3.30 \end{pmatrix} \begin{pmatrix} 0.75 \\ 0 \\ 0.25 \\ 0 \end{pmatrix}$$

$$Z_1 = (0.50 \times 0.75) + (0.54 \times 025) = 0.51$$

$$Z_2 = (1.00 \times 0.75) + (1.00 \times 0.25) = 1$$

$$Z_3 = (2.00 \times 0.75) + (1.60 \times 0.25) = 1.90$$

$$Z_4 = (400 \times 0.75) + (3.50 \times 0.25) = 3.875 \tag{44}$$

Control point C_{13}

$$\begin{pmatrix} Z_1 \\ Z_2 \\ Z_3 \\ Z_4 \end{pmatrix} = \begin{pmatrix} 0.50 & 0.52 & 0.54 & 0.56 \\ 1.00 & 1.00 & 1.00 & 1.00 \\ 2.00 & 1.80 & 1.60 & 1.40 \\ 4.00 & 3.70 & 3.50 & 3.30 \end{pmatrix} \begin{pmatrix} 0 \\ 0.5 \\ 0.25 \\ 0.25 \end{pmatrix}$$

$$Z_1 = (0.52 \times 0.5) + (0.54 \times 02.5) + (0.56 \times 0.25) = 0.535$$

$$Z_2 = (1.00 \times 0.5) + (1.00 \times 0.25) + (0.00 \times 0.25) = 1$$

$$Z_3 = (1.80 \times 0.5) + (1.60 \times 0.25) + (1.4 \times 0.25) = 1.65$$

$$Z_4 = (3.70 \times 0.5) + (3.50 \times 0.25) + (3.3 \times 0.25) = 3.55 \tag{45}$$

Control Point C_{14}

$$\begin{pmatrix} Z_1 \\ Z_2 \\ Z_3 \\ Z_4 \end{pmatrix} = \begin{pmatrix} 0.50 & 0.52 & 0.54 & 0.56 \\ 1.00 & 1.00 & 1.00 & 1.00 \\ 2.00 & 1.80 & 1.60 & 1.40 \\ 4.00 & 3.70 & 3.50 & 3.30 \end{pmatrix} \begin{pmatrix} 0.25 \\ 0 \\ 0.50 \\ 0.25 \end{pmatrix}$$

$$Z_1 = (0.50 \times 0.25) + (0.54 \times 0.5) + (0.56 \times 0.25) = 0.535$$

$$Z_2 = (1.00 \times 0.25) + (1.00 \times 0.5) + (1.00 \times 0.25) = 1$$

$$Z_3 = (2.00 \times 0.25) + (1.60 \times 0.5) + (1.40 \times 0.25) = 1.65$$

$$Z_4 = (4.60 \times 0.25) + (3.5 \times 0.5) + (3.30 \times 0.25) = 3.575 \tag{46}$$

Control Point C_{23}

$$\begin{pmatrix} Z_1 \\ Z_2 \\ Z_3 \\ Z_4 \end{pmatrix} = \begin{pmatrix} 0.50 & 0.52 & 0.54 & 0.56 \\ 1.00 & 1.00 & 1.00 & 1.00 \\ 2.00 & 1.80 & 1.60 & 1.40 \\ 4.00 & 3.70 & 3.50 & 3.30 \end{pmatrix} \begin{pmatrix} 0.75 \\ 0.25 \\ 0 \\ 0 \end{pmatrix}$$

$$Z_1 = (0.50 \times 0.75) + (0.52 \times 025) = 0.505$$

$$Z_2 = (1.00 \times 0.75) + (1.00 \times 0.25) = 1$$

$$Z_3 = (2.00 \times 0.75) + (1.80 \times 0.25) = 1.95$$

$$Z_4 = (400 \times 0.75) + (3.70 \times 0.25) = 3.925 \tag{47}$$

Control point C_{24}

$$\begin{pmatrix} Z_1 \\ Z_2 \\ Z_3 \\ Z_4 \end{pmatrix} = \begin{pmatrix} 0.50 & 0.52 & 0.54 & 0.56 \\ 1.00 & 1.00 & 1.00 & 1.00 \\ 2.00 & 1.80 & 1.60 & 1.40 \\ 4.00 & 3.70 & 3.50 & 3.30 \end{pmatrix} \begin{pmatrix} 0 \\ 0.75 \\ 0.25 \\ 0 \end{pmatrix}$$

$$Z_1 = (0.52 \times 0.75) + (0.54 \times 025) = 0.525$$

$$Z_2 = (1.00 \times 0.75) + (1.00 \times 0.25) = 1$$

$$Z_3 = (1.80 \times 0.75) + (1.60 \times 0.25) = 1.75$$

$$Z_4 = (3.70 \times 0.75) + (3.50 \times 0.25) = 3.65 \tag{48}$$

Control point C_{34}

$$\begin{pmatrix} Z_1 \\ Z_2 \\ Z_3 \\ Z_4 \end{pmatrix} = \begin{pmatrix} 0.50 & 0.52 & 0.54 & 0.56 \\ 1.00 & 1.00 & 1.00 & 1.00 \\ 2.00 & 1.80 & 1.60 & 1.40 \\ 4.00 & 3.70 & 3.50 & 3.30 \end{pmatrix} \begin{pmatrix} 0 \\ 0.4 \\ 0.4 \\ 0.2 \end{pmatrix}$$

$$Z_1 = (0.52 \times 0.4) + (0.54 \times 0.4) + (0.56 \times 0.2) = 0.536$$

$$Z_2 = (1.00 \times 0.4) + (1.00 \times 0.4) + (1.00 \times 0.2) = 1$$

$$Z_3 = (1.80 \times 0.4) + (1.60 \times 0.4) + (1.4 \times 0.2) = 1.64$$

$$Z_4 = (3.70 \times 0.4) + (3.50 \times 0.4) + (3.3 \times 0.2) = 3.54 \quad (48)$$

The pseudo components and the corresponding actual components are summarized in Table 4.

Table 4. Mixture proportions of control points

	Actual					Pseudo			
S/N	Z_1	Z_2	Z_3	Z_4	Response	x_1	x_2	x_3	x_4
1	0.53	1	170	3.625	C_1	0.25	0.25	0.25	0.25
2	0.515	1	1.85	3.80	C_2	0.50	0.25	0.25	0
3	0.545	1	1.55	3.45	C_3	0	0.25	0.25	0.50
4	0.55	1	1.50	3.40	C_4	0	0.25	0	0.75
5	0.51	1	1.90	3.875	C_{12}	0.75	0	0.25	0
6	0.535	1	1.65	3.55	C_{13}	0	0.50	0.25	0.25
7	0.535	1	1.65	3.575	C_{14}	0.25	0	0.50	0.25
8	0.505	1	1.95	3.925	C_{23}	0.75	0.25	0	0
9	0.505	1	1.75	3.65	C_{24}	0	0.75	0.25	0
10	1.536	1	1.64	3.54	C_{34}	0	0.40	0.40	0.20

3. Results and discussion

3.1 *Result on materials testing laboratory*

In the pursuit of understanding the mechanical and material properties crucial to construction, a series of rigorous experiments and analyses were conducted in the Materials Testing Laboratory. This section presents a detailed account of the findings obtained through a variety of tests, each shedding light on different facets of the materials involved. Commencing with the fine aggregate, Figure 2 provides a comprehensive sieve analysis, delineating the particle size distribution and characteristics of the material. While Tables 5-7 present the specific gravity of the specimens, crushing test of Concrete for Zone IV and Zone III, respectively. This analysis serves as a foundational exploration, unveiling key insights into the gradation of the fine aggregate (Ibagwa sand).

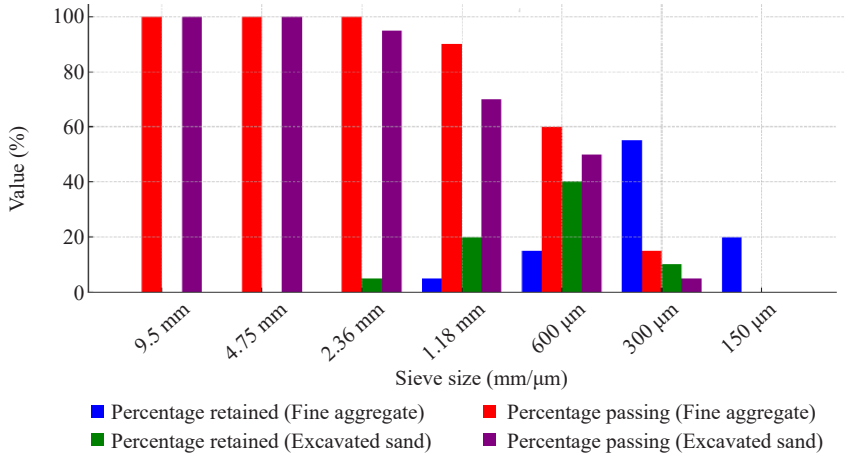

Figure 2. Comparative sieve analysis of fine aggregate and excavated

Table 5. Specific gravity of fine aggregate and coarse aggregate (20 mm)

Measurement	Fine aggregate (Bottle A)	Fine aggregate (Bottle B)	Coarse aggregate (Bottle A)	Coarse aggregate (Bottle B)
Empty weight of psychomotor (g)	462.5	462.4	462.5	462.4
Empty weight + sample (g)	940	904.9	1,101.7	1,087.4
Sample weight: K-X (g)	477.5	447.5	639.2	625
Empty weight + sample + water (g)	1,799.9	1,905.8	2,001.8	1,995.8
Empty weight + water (g)	1,596	1,603	1,592	1,602
Oven dry sample weight (g)	517.7	472.7	688.6	674.5
Saturated surface dry (SSD)	1.75	3.17	2.79	2.7
SSD average	7.46		2.75	
Oven dry basis	1.89	1.56	3	2.92
OD average	1.73		2.96	

As presented in Figure 2, the sieve analysis results reveal notable differences between the fine aggregate and the excavated sand. The fine aggregate shows minimal retention at larger sieve sizes, with 0.00% retained at 9.5 mm and only 0.61% at 4.75 mm, leading to a high percentage passing through these sieves (100.00% and 99.39%, respectively). In contrast, the excavated sand retains 0.17% and 1.67% at these same sieve sizes, resulting in slightly lower passing percentages (99.83% and 98.16%). The disparity becomes more pronounced at smaller sieve sizes, with the fine aggregate retaining 22.53% at 600 µm and 54.94% at 300 µm, while the excavated sand retains significantly more at 57.90% and only 9.55% at 600 µm and 300 µm, respectively.

Similar result was observed from the research conducted by Akobo et al. [35] on optimization of compressive strength of concrete containing rubber chips as coarse aggregate. These results indicate that the fine aggregate has a finer particle distribution compared to the excavated sand, which suggests that it may be more suitable for applications requiring smoother finishes. The implications of this analysis are crucial for selecting appropriate materials for specific construction needs, ensuring optimal performance and durability.

As presented in Table 5, the specific gravity results for both fine and coarse aggregates show significant variations. The fine aggregate's saturated surface dry (SSD) values, especially for Bottle B at 3.17, are notable, indicating higher water absorption. Coarse aggregate's oven dry (OD) Basis values are consistently higher, with an average of 2.96, compared to fine aggregate's average of 1.73. This implies that coarse aggregate is denser, contributing to a stronger and more durable concrete mix. Therefore, the coarse aggregate is more suitable for structural applications where higher strength is essential. These results highlight the importance of specific gravity in determining material quality and suitability for construction purposes, as highlighted on the research by Alaneme and Mbadike [36], on optimization of flexural strength of palm nut fibre concrete using Scheffe's theory.

As presented in Tables 6-7, the compressive strength tests reveal a significant difference between the concrete samples from Zone III and Zone IV. Zone III samples exhibited higher compressive strength values, averaging 22.22 N/mm^2, compared to Zone IV's average of 13.48 N/mm^2. The best individual value was observed in Zone III, Test 2, with a compressive strength of 24.44 N/mm^2. This suggests that the concrete mix from Zone III is more robust and suitable for applications requiring higher strength. Similar results were observed by Ambrose et al. [10] in their study on the compressive strength and workability of laterized quarry sand concrete. These findings suggest that materials from Zone III provide superior performance in structural applications, making them preferable for critical construction projects.

Table 6. Crushing test of concrete for Zone IV

S/No	Test No.	1	2	3	Average
1	Specimen size	150 mm	150 mm	150 mm	
2	Age (Days)	7	7	7	
3	Date of mix		28/1/22		
4	Date of test		4/2/22		
5	Appearance		SMOOTH		
6	Curing condition		POOLING		
7	Weight of specimen (kg)	6,884 g	7,135 g	7,082 g	
8	Type of fracture		SHEAR		
9	Load of ram (KN)	220	340	350	
10	Compressive strength N/mm^2	9.78	15.11	15.56	13.48

Table 7. Crushing test of concrete for Zone III

S/NO	Test No.	1	2	3	Average
1	Specimen size	150 mm	150 mm	150 mm	
2	Age (Days)	7	7	7	
3	Date of mix		29/1/22		
4	Date of test		5/2/22		
5	Appearance		SMOOTH		
6	Curing condition		POOLING		
7	Weight of specimen (kg)	7,735 g	7,827 g	7,860 g	
8	Type of fracture		SHEAR		
9	Load of ram (KN)	460	550	490	
10	Compressive strength N/mm^2	20.44	24.44	21.78	22.22

3.2 *Model results*

Tables 8 and 9 present the 28-day compressive strength results for the response (Y_1) and control points using Zone III sand. Compressive strength values, crushing loads, and area measurements are crucial parameters for evaluating the structural performance of concrete mixtures.

As presented in Table 8, the values of the compressive strength of concrete for the Zone III sand at 28 days curing age were obtained using the Scheffe's model formulated in equation (11). The highest compressive strength values of 28.45 N/mm^2 corresponding to a mix ratio of 0.50 : 1 : 2 : 4 was obtained while the lowest compressive strength was found to be 25.89 N/mm^2 corresponding to a mix ratio of 0.56 : 1 : 1 : 4 : 3.30 for water, cement, sand and crushed granite respectively. The result showed that the formulated model can be used to predict the compressive strength of C25 concrete, similar result was observed from the research conducted by Ubachukwu and Okafor [31], on the formulation of predictive model for the compressive strength of oyster shell powder-cement concrete using Scheffe's simplex lattice

theory.

Table 8. 28-day compressive strength results for the response (Y_1) using Zone III sand

Response	Replicate	Average weight (kg)	Volume (m^3)	Average bulk density	Crushing load (N)	Area (mm^2)	Compressive strength	Average compressive strength
Y_1	A B	8.12	0.003375	2,405.93	645,000 635,000	22,500	28.67 28.22	28.45
Y_2	A B	8.07	0.003375	2,391.11	617,000 593,000	22,500	27.42 26.36	26.89
Y_3	A B	7.93	0.003375	2,349.63	605,000 591,000	22,500	26.89 26.27	26.58
Y_4	A B	7.87	0.003375	2,331.82	580,000 585,000	22,500	25.78 26.00	25.89
Y_{12}	A B	8.09	0.003375	2,397.04	630,000 635,000	22,500	28.00 28.22	28.11
Y_{13}	A B	8.03	0.003375	2,379.26	616,000 608,000	22,500	27.37 27.02	27.20
Y_{14}	A B	7.91	0.003375	2,343.70	590,000 610,000	22,500	26.22 27.11	26.67
Y_{23}	A B	7.90	0.003375	2,346.74	605,000 593,000	22,500	26.89 26.36	26.63
Y_{24}	A B	7.84	0.003375	2,322.96	590,000 600,000	22,500	26.22 26.67	26.45
Y_{34}	A B	7.90	0.003375	2,311.11	585,000 588,000	22,500	26.00 26.13	26.07

Table 9. 28-day compressive strength results for the control points using Zone III sand

Response	Replicate	Average weight	Volume (m^3)	Average bulk density	Crushing load (N)	Area (mm^2)	Compressive strength (N/mm^2)	Average compressive strength
C_1	A B	7.95	0.003375	2,355.56	592,000 601,500	22,500	26.31 26.73	26.52
C_2	A B	8.08	0.003375	2,394.07	603,000 607,500	22,500	26.80 27.00	26.90
C_3	A B	7.83	0.003375	2,320.00	597,200 587,000	22,500	26.54 26.09	26.27
C_4	A B	7.80	0.003375	2,311.11	584,000 590,000	22,500	25.96 26.22	26.09
C_{12}	A B	7.10	0.003375	2,400.00	632,000 635,000	22,500	28.09 28.22	28.15
C_{13}	A B	8.04	0.003375	2,382.22	605,500 596,000	22,500	26.91 26.49	26.70
C_{14}	A B	7.97	0.003375	2,361.48	600,000 604,000	22,500	26.67 26.84	26.75
C_{23}	A B	8.15	0.003375	244.81	639,000 643,600	22,500	28.40 28.60	38.50
C_{24}	A B	7.88	0.003375	2,334.81	599,000 600,300	22,500	26.62 26.68	26.65
C_{34}	A B	7.84	0.003375	2,322.96	597,200 590,000	22,500	26.54 26.22	26.38

Also in Table 9, the compressive strength values for Zone IV sand concrete at a 28-day curing age were obtained

using Scheffe's model, as formulated in equation (26). The highest compressive strength value of 27.89 N/mm^2 corresponding to a mix ratio of 0.505 : 1 : 1.95 : 3.925 was obtained, while the lowest compressive strength was found to be 24.78 N/mm^2 corresponding to a mix ratio of 0.56 : 1 : 4 : 3.30 for water, cement, sand, and crushed granite, respectively. The results showed that the formulated model can be used to predict the compressive strength of C20 concrete, consistent with research conducted by Enang and Ewa [16] on mixture experiment model for predicting static modulus of elasticity of laterite-quarry dust cement block. A comparative analysis is provided in Figure 3, showcasing the experimental test results alongside Scheffe's model test results for various responses.

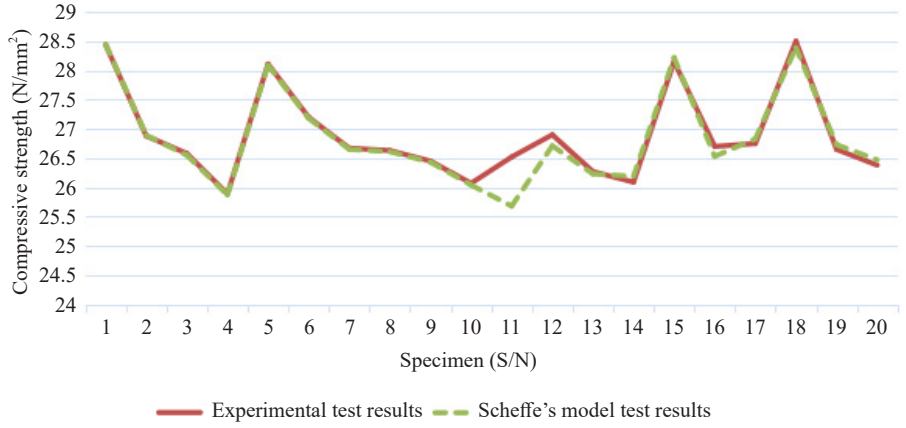

Figure 3. Experimental test results and Scheffe's model tests comparison of the compressive strength results

Discrepancies or agreements between experimental and model results are highlighted in Figure 3, providing a comprehensive understanding of the experimental result from the compressive strength data and that of applied predictive model. From the obtained, both trends are closely aligned showing that the data are closely inline observing underfitting and overfitting. This trend indicates the effeteness of Scheffe's model in data analysis, as also relatively conducted by Agunwamba et al. in their study [34] on application of Scheffe's simplex lattice model for concrete mixture design and performance enhancement.

3.2.1 *Validation of the experimental and the applied model*

As presented in Tables 10-11, Fisher's test was used to validate the adequacy of the model. The null hypothesis (Fcal > Fcritical) was tested, and the results showed Fcal = 1.297 and Fcritical = 3.18, i.e., Fcal < Fcritical. This indicates that the null hypothesis is accepted, as there was no significant difference between the experimental test results and the model predictions. Therefore, the model is adequate.

As presented in Tables 10 and 11, Fisher's test results for concrete produced with Zone III and Zone IV sands show varying degrees of alignment between the experimental and model results. For Zone III sand, minimal differences are observed, with the highest variance in specimen C_{12} (experimental: 1.18, model: 1.32). The total sums of squares for experimental and model variances are 5.398 and 7.002, respectively. Similar validation results were observed in the application of Scheffe's model for optimizing the compressive strength of lateritic concrete in the study of Mbadike and Osadebe [38], which observed a good degree of fitting from the validation. This indicates a reliable prediction model. In contrast, results for Zone IV sand exhibit greater variances, with the highest deviations in specimen C_{23} (experimental: 1.48, model: 1.40) and total sums of squares of 5.26 and 6.80, respectively. This suggests a need for further model refinement for Zone IV applications.

Table 10. Fisher's test result for concrete produced using Zone III sand

	γ_e	γ_m	$\gamma_e - \gamma_{ee}$	$\gamma_m - \gamma_{mm}$	$(\gamma_e - \gamma_{ee})^2$	$(\gamma_m - \gamma_{mm})^2$
C_1	26.52	25.68	-0.45	-1.22	0.203	1.488
C_2	26.90	27.71	-0.07	0.81	0.005	0.656
C_3	26.27	26.23	-0.43	-0.67	0.185	0.449
C_4	26.09	26.19	-0.88	-0.71	0.774	0.121
C_{12}	28.15	28.22	1.18	1.32	1.392	1.742
C_{13}	26.70	26.63	-0.27	-0.37	0.075	0.137
C_{14}	26.75	26.83	0.22	-0.07	0.048	0.005
C_{23}	28.50	25.39	1.53	1.49	0.341	2.190
C_{24}	26.65	26.73	-0.82	-0.17	0.102	0.029
C_{34}	26.36	26.47	-0.52	-0.43	0.27	0.185
Total	268.89	266.08			3.395	7.002
Mean	26.99	26.61				

Table 11. Fisher's test result for concrete produced using Zone IV sand

	Y_2	Y_m	$Y_e - Y_e$	$Y_m - Y_{mm}$	$(y_e - y_{ee})^2$	$(Y_m - Y_{mm})^2$
C_1	26.33	25.74	-0.08	-0.07	0.01	0.00
C_2	26.85	26.77	0.44	0.96	0.19	-0.82
C_3	25.83	24.92	-0.58	-0.89	0.34	0.79
C_4	25.45	24.81	-0.96	-1.00	0.92	1.00
C_{12}	27.45	26.96	1.04	1.15	1.08	1.32
C_{13}	25.91	25.20	-0.50	-0.61	0.25	0.37
C_{14}	26.00	25.64	-0.41	-0.17	0.17	0.03
C_{23}	27.89	22.25	1.48	1.40	2.19	1.96
C_{24}	26.29	25.64	-0.12	-0.17	0.01	0.03
C_{34}	26.09	25.19	-0.32	-0.62	0.10	0.38
Total	264.09	253.12			5.26	5.06
Mean	26.409	25.312				

4. Conclusion

This study focused on optimizing the compressive strength of concrete by analyzing sand characteristics from two distinct zones using Scheffe's model. The model effectively predicted and optimized the compressive strength, with validation through Fisher's test confirming its reliability and accuracy. The comparative analysis demonstrated that Zone III sand exhibited a higher compressive strength (22.22 N/mm^2) compared to Zone IV sand (13.48 N/mm^2),

underscoring the significant impact of sand quality on concrete performance. The findings highlight the importance of selecting appropriate fine aggregate materials to achieve the desired concrete strength. However, the study is limited to compressive strength and does not account for other mechanical or durability properties, which could be explored in future research. These insights provide valuable guidance for material selection in construction, contributing to the development of sustainable and reliable concrete formulations.

Authors' contributions

This work was carried out in collaboration between all authors. Authors DAE, OVC, and UVO sourced and collected the required materials. JDO, OCO, EIN, and HA prepared the specimens. UVO, VCE, and ENI conducted the laboratory experiments. HA, OVC, and DAE ran the model analysis. CAN, JBO, and DAE wrote the protocol and the first draft of the manuscript. Authors DAE, EIN, and OVC managed the literature searches. All authors read and approved the final manuscript.

Conflict of interest

The authors declare no conflict of interest.

References

[1] E. E. Ikponmwosa and S. O. Ehikhuenmen, "The effect of ceramic waste as coarse aggregate on strength properties of concrete," *Nigerian Journal of Technology*, vol. 36, no. 3, pp. 691-696, 2017.

[2] Z. Tahar, B. Benabed, E. L. H. Kadri, T. T. Ngo, and A. Bouvet, "Rheology and strength of concrete made with recycled concrete aggregate as replacement of natural aggregates," *Epitoanyag Journal of Silicate Based and Composite Materials*, vol. 72, no. 2, pp. 48-58, 2020.

[3] P. Domone and J. Illston, *Construction Materials-The Nature and Behaviour*. CRC Press, 2010.

[4] E. Gartner, "Industrial interesting approaches to low CO_2," *Cement and Concrete Research*, vol. 34, no. 9, pp. 1489-1498, 2004.

[5] A. M. Neville, *Properties of Concrete*. London: Pearson Education, 2011.

[6] A. Allahverdi, M. Mahinroosta, and S. Pilehvar, "A temperature-age model for prediction of compressive strength of chemically activated high phosphorus slag content cement," *International Journal of Civil Engineering*, vol. 15, no. 5, pp. 839-847, 2017.

[7] V. Okpalaku-Nath, J. Okpuzor, and D. Ekpechi, "A review on bacteria based self-healing concrete," *International Journal of Innovation Scientific Research and Review*, vol. 4, no. 1, pp. 2454-1362, 2021.

[8] D. M. Kannan, S. H. Aboubakr, A. S. El-Dieb, and M. M. R. Taha, "High performance concrete incorporating ceramic wastes powder as large partial replacement of Portland cement," *Construction and Building Materials*, vol. 144, pp. 35-41, 2017.

[9] W. C. Tang, Y. Lo, and A. Nadeem, "Mechanical and dryness shrinkage properties of structural-graded polystyrene aggregate concrete," *Cement and Concrete Composites*, vol. 30, no. 5, pp. 403-409, 2008.

[10] E. E. Ambrose, D. U. Ekpo, I. M. Umoren, and U. S. Ekwere, "Compressive strength and workability of laterized quarry sand concrete," *Nigerian Journal of Technology*, vol. 36, no. 3, pp. 605-610, 2018.

[11] H. Elci, "Utilization of crushed floor and wall tile wastes as aggregate in concrete production," *Journal of Cleaner Production*, vol. 112, no. 1, pp. 742-752, 2016.

[12] E. E. A. Edidiong, F. O. Okafor, and M. E. Onyia, "Compressive strength and Scheffe's optimization of mechanical properties of recycled ceramics tile aggregate concrete," *Journal of Silicate Based and Composite Materials*, vol. 73, no. 3, pp. 91-102, 2020.

[13] P. O. Awoyera, J. M. Ndambuki, J. O. Akinmusuru, and David O. Omole, "Characterization of ceramic waste aggregate," *HBRC Journal*, vol. 14, no. 3, pp. 282-287, 2018.

[14] G. A. Akeke, P. E. U. Inem, G. U. Alaneme, and E. E. Nyah, "Experimental investigation and modelling of the mechanical properties of palm oil fuel ash concrete using Scheffe's method," *Scientific Reports*, vol. 13, pp. 18583,

2023.
[15] O. Zimbili, W. Salim, and M. Ndambuki, "A review on the usage of ceramic wastes in concrete production," *International Journal of Civil, Environmental, Structural, Construction and Architectural Engineering*, vol. 8, no. 1, pp. 91-99, 2014.
[16] E. Enang and E. Ewa, "Mixture experiment model for predicting static modulus of elasticity of laterite-quarry dust cement block," *Saudi Journal of Civil Engineering*, vol. 6, no. 4, pp. 72-78, 2022.
[17] M. C. Arimanwa, D. O. Onwuka, and J. I. Arimanwa, "Effect of chemical composition of ordinary Portland cement on the compressive strength of concrete," *International Refereed Journal of Engineering and Science (IRJES)*, vol. 5, no. 3, pp. 20-31, 2016.
[18] F. Mulizar, A. Iskandar, and A. Fauzi, "Effect of POFA as a replacement material on fly ash based geopolymer mortar," *IOP Conference Series: Materials Science and Engineering*, vol. 854, no. 1, pp. 012012, 2020.
[19] J. K. Prusty and B. Pradhan, "Multi-response optimization using Taguchi-Grey relational analysis for composition of fly ash-ground granulated blast furnace slag based geopolymer concrete," *Construction and Building Materials*, vol. 241, pp. 118049, 2020.
[20] J. Sengupta, N. Dhang, and A. Deb, "Efficient mix design of one-part alkali-activated concrete using packing density method and its optimization through Taguchi-GRA," *Construction and Building Materials*, vol. 438, pp. 136869, 2024.
[21] U. A. George, and E. M. Elvis, "Optimization of flexural strength of palm nut fibre concrete using Scheffe's theory," *Materials Science for Energy Technologies*, vol. 2, no. 2, pp. 272-287, 2019.
[22] A. Habibi, A. M. Ramezanianpour, and M. Mahdikhani, "RSM-based optimized mix design of recycled aggregate concrete containing supplementary cementitious materials based on waste generation and global warming potential," *Resources, Conservation and Recycling*, vol. 167, pp. 105420, 2021.
[23] K. Siamardi, "Optimization of fresh and hardened properties of structural lightweight self-compacting concrete mix design using response surface methodology," *Construction and Building Materials*, vol. 317, pp. 125928, 2022.
[24] H. Scheffé, "The simplex-centroid design for experiments with mixtures," *Journal of the Royal Statistical Society: Series B (Methodological)*, vol. 25, no. 2, pp. 235-251, 1963.
[25] E. M. Mbadike and N. N. Osadebe, "Application of Scheffe's model in optimization of compressive strength of lateritic concrete," *Journal of Engineering and Applied Sciences*, vol. 9, no. 1, pp. 17-23, 2013.
[26] M. E. Onyia, E. E. Ambrose, F. O. Okafor, and J. J. Udo, "Mathematical modelling of compressive strength of recycled ceramic tile aggregate concrete using modified regression theory," *Journal of Applied Sciences and Environmental Management*, vol. 27, no. 1, pp. 33-42, 2023.
[27] I. C. Attah, R. K. Etim, G. U. Alaneme, D. U. Ekpo, and I. N. Usanga, "Scheffe's approach for single additive optimization in selected soils amelioration studies for cleaner environment and sustainable subgrade materials," *Cleaner Materials*, vol. 4, pp. 100126, 2022.
[28] G. A. Akeke, P. E. U. Inem, G. U. Alaneme, and E. E. Nyah, "Experimental investigation and modelling of the mechanical properties of palm oil fuel ash concrete using Scheffe's method," *Scientific Reports*, vol. 13, no. 1, pp. 18583, 2023.
[29] G. Alaneme and E. Mbadike, "Modelling of the compressive strength of palm-nut-fibre concrete using Scheffe's theory," *Computational Engineering and Physical Modeling*, vol. 3, no. 1, pp. 31-40, 2020.
[30] I. C. Attah, R. K. Etim, G. U. Alaneme, and O. B. Bassey, "Optimization of mechanical properties of rice husk ash concrete using Scheffe's theory," *SN Applied Sciences*, vol. 2, pp. 928, 2020.
[31] O. A. Ubachukwu and F. O. Okafor, "Formulation of predictive model for the compressive strength of oyster shell powder-cement concrete using Scheffe's simplex lattice theory," *Journal of Silicate Based and Composite Materials*, vol. 72, no. 6, pp. 210-218, 2020.
[32] E. E. Ambrose, F. O. Okafor, and M. E. Onyia, "Compressive strength and Scheffe's optimization of mechanical properties of recycled ceramics tile aggregate concrete," *Epitoanyag-Journal of Silicate Based and Composite Materials*, vol. 73, no. 3, pp. 91-102, 2021.
[33] K. Onyelowe, G. Alaneme, C. Igboayaka, F. Orji, H. Ugwuanyi, D. B. Van, and M. N. Van, "Scheffe optimization of swelling, California bearing ratio, compressive strength, and durability potentials of quarry dust stabilized soft clay soil," *Material Science for Energy Technology*, vol. 2, no. 1, pp. 67-77, 2019.
[34] J. Agunwamba, F. Okafor, and M. T. Tiza, "Application of Scheffe's simplex lattice model in concrete mixture design and performance enhancement," *Environmental Research and Technology*, vol. 7, no. 2, pp. 270-279, 2024.
[35] I. Z. Akobo, S. B. Akpila, and B. Okedeyi, "Optimization of compressive strength of concrete containing rubber chips as coarse aggregate based on Scheffe's model," *International Journal of Civil Engineering*, vol. 7, no. 7, pp.

93-110, 2020.
[36] G. U. Alaneme and E. Mbadike, "Optimization of flexural strength of palm nut fibre concrete using Scheffe's theory," *Materials Science for Energy Technologies*, vol. 2, no. 2, pp. 272-287, 2019.
[37] J. I. Arimanwa, D. O. Onwuka, M. C. Arimanwa, and U. S. Onwuka, "Prediction of the compressive strength of aluminum waste-cement concrete using Scheffe's theory," *Journal of Materials in Civil Engineering*, vol. 24, no. 2, pp. 177-183, 2012.
[38] E. M. Mbadike and N. N. Osadebe, "Application of Scheffe's model in optimization of compressive strength of lateritic concrete," *Journal of Civil Engineering and Construction Technology*, vol. 4, no. 9, pp. 265-274, 2013.